Check for updates

the plant journal

SEB SOCIETY FOR EXPERIMENTAL BIOLOGY

The Plant Journal (2024) **119,** 2045–2062 doi: 10.1111/tpj.16909

Carbon usage in yellow-fleshed *Manihot esculenta* storage roots shifts from starch biosynthesis to cell wall and raffinose biosynthesis via the *myo*-inositol pathway

Sindy Gutschker[1], David Ruescher[1], Ismail Y. Rabbi[2], Laise Rosado-Souza[3], Benjamin Pommerrenig[4], Markus Pauly[5], Stefan Robertz[5], Anna M. van Doorn[2], Armin Schlereth[3], H. Ekkehard Neuhaus[4], Alisdair R. Fernie[3], Stephan Reinert[1], Uwe Sonnewald[1] and Wolfgang Zierer[1,*]

[1]*Friedrich-Alexander-Universität Erlangen-Nürnberg, Division of Biochemistry, Erlangen, Germany,*
[2]*International Institute of Tropical Agriculture, Ibadan, Nigeria,*
[3]*Max Planck Institute of Molecular Plant Physiology, Potsdam, Germany,*
[4]*University of Kaiserslautern, Plant Physiology, Kaiserslautern, Germany, and*
[5]*Heinrich-Heine-University, Institute of Plant Cell Biology and Biotechnology, Düsseldorf, Germany*

Received 29 November 2023; revised 17 June 2024; accepted 20 June 2024; published online 3 July 2024.
*For correspondence (e-mail wolfgang.zierer@fau.de).

SUMMARY

Cassava is a crucial staple crop for smallholder farmers in tropical Asia and Sub-Saharan Africa. Although high yield remains the top priority for farmers, the significance of nutritional values has increased in cassava breeding programs. A notable negative correlation between provitamin A and starch accumulation poses a significant challenge for breeding efforts. The negative correlation between starch and carotenoid levels in conventional and genetically modified cassava plants implies the absence of a direct genomic connection between the two traits. The competition among various carbon pathways seems to account for this relationship. In this study, we conducted a thorough analysis of 49 African cassava genotypes with varying levels of starch and provitamin A. Our goal was to identify factors contributing to differential starch accumulation. Considering carotenoid levels as a confounding factor in starch production, we found that yellow- and white-fleshed storage roots did not differ significantly in most measured components of starch or *de novo* fatty acid biosynthesis. However, genes and metabolites associated with *myo*-inositol synthesis and cell wall polymer production were substantially enriched in high provitamin A genotypes. These results indicate that yellow-fleshed cultivars, in comparison to their white-fleshed counterparts, direct more carbon toward the synthesis of raffinose and cell wall components. This finding is underlined by a significant rise in cell wall components measured within the 20 most contrasting genotypes for carotenoid levels. Our findings enhance the comprehension of the biosynthesis of starch and carotenoids in the storage roots of cassava.

Keywords: *Manihot esculenta*, cassava, starch content, carotenoid content, *myo*-inositol, cell wall components, raffinose, provitamin A.

INTRODUCTION

Manihot esculenta, also known as cassava, is one of the most widely cultivated crops in tropical and subtropical regions of the world, particularly in Asia and Sub-Saharan Africa, where it serves as food for millions of people (Carvalho et al., 2018; FAO, 2023). It is a source of carbohydrates, vitamins, and minerals, and despite the economic and nutritional importance of cassava, the yield potential of this crop has not yet been fully realized. Low productivity levels are still a major challenge faced by smallholder farmers in Sub-Saharan Africa, leading to concerns about food security, especially in the face of climate change and a growing population. Cassava breeding programs typically prioritize the enhancement of fresh root yield and starch content due to their demonstrable influence on the adoption of new cultivars (Awotide et al., 2014). The most widely consumed cassava storage roots around the world are white fleshed and starch rich but possess low levels of micronutrients, especially provitamin A (Welsch et al., 2010). Vitamin A deficiency (VAD), however, remains a prevalent problem, especially in Sub-Saharan Africa, leading not only to the deterioration of vision and even

© 2024 The Author(s).
The Plant Journal published by Society for Experimental Biology and John Wiley & Sons Ltd.
This is an open access article under the terms of the Creative Commons Attribution License, which permits use, distribution and reproduction in any medium, provided the original work is properly cited.

blindness but also to a weakened immune system and slow growth in children.

Therefore, genetic improvement of cassava for nutritional attributes such as provitamin A is an additional target in breeding projects, intended to simultaneously address nutritional deficits (Hefferon, 2015; Nassar & Ortiz, 2010; Talsma et al., 2018). Initial efforts on cassava breeding aimed to enhance carotenoid or dry matter content focusing on the identification and characterization of useful genetic variants (Chavez et al., 2000; Iglesias et al., 1997). Welsch et al. (2010) unveiled that a $C_{572}A$ nucleotide substitution in phytoene synthase 2 (PSY2), a key regulator in the carotenoid biosynthesis pathway, is responsible for the qualitative color of yellow-fleshed cassava roots with additive genetic effect (AA > AC > CC). Furthermore, the authors demonstrated that this allelic variation in *PSY2* increases the activity of the enzyme and therefore contributes to the increased carotenoid accumulation. Subsequently, two primary loci responsible for storage root yellowness were identified by genome-wide association study (GWAS) (Rabbi et al., 2017). The authors also identified one yellowness locus that is co-located with a unique dry matter locus suggesting that the observed negative correlation between starch and carotenoid content might arise from physical linkage of these two loci and the allelic status of candidate genes localized within these regions (Rabbi et al., 2017). Phenotypic analysis of African cassava storage roots also elucidated that increased carotenoid concentrations in different cultivars correlate with reduced starch accumulation, while high-carotenoid varieties still show high variations in starch accumulation levels (Esuma et al., 2016; Njoku et al., 2015; Rabbi et al., 2017; Rabbi et al., 2022).

Several studies examined expression or metabolite patterns in high-starch or high-carotenoid genotypes (Beyene et al., 2018; Cai et al., 2023; Luo et al., 2023; Ogbonna et al., 2021; Olayide et al., 2023; Wilson et al., 2017; Xiao et al., 2021). Beyene et al. (2018), for example, performed carotenoid enrichment research and successfully increased β-carotene content in cassava roots by co-expression of transgenes for *deoxy-D-xylose-5-phosphate synthase* (*DXS*) and bacterial *phytoene synthase* (*crtB*), both known to play pivotal roles in carotenoid biosynthesis. This resulted in a reduction of the dry matter content by 50 to 60% when compared to the non-transgenic controls and increased the concentrations of soluble sugars and triacylglycerols in the examined storage roots, especially within the ones showing the highest carotenoid levels. Olayide et al. (2023) examined the transcriptome of 11 cassava genotypes with root colors ranging from white to deep yellow and could not observe a relationship between the expression of genes in the carotenoid biosynthesis pathway and the root's yellowness. They hypothesized that starch and carotenoid biosynthesis might compete for glyceraldehyde-3-phosphate (GA3P). GA3P not only initiates the methyl-D-erythritol phosphate (MEP) pathway to produce precursors for β-carotene synthesis but is also converted to D-glucose-1-phosphate (G1P) in the starch biosynthesis pathway. In sink organs, however, most of the G1P for starch synthesis is not generated through triose phosphate, but through the cleavage of arriving sucrose into hexose phosphates. Olayide et al. (2023) could not detect clear differences in the expression profiles of genes significantly expressed in roots and involved in glycolysis between high-starch and high-carotenoid genotypes. It is not yet fully understood why the increased accumulation of carotenoids reduces starch accumulation in the high-carotenoid genotypes and how their carbon allocation differs from the high-starch/low-carotenoid varieties.

To better understand the molecular basis of the competition between starch and carotenoid accumulation, we investigated 49 field-grown African cassava genotypes, with contrasting starch and carotenoid levels. We identified the transcript and metabolite patterns for high-starch/low-carotenoid (in the following referred to as "white" genotypes) and low-starch/high-carotenoid varieties (hereafter termed "yellow" genotypes) that were directly linked to the varieties' starch content and showed that both groups had similar patterns in carbon allocation strategies for sucrose breakdown and starch accumulation, or *de novo* biosynthesis of fatty acids. However, storage roots of yellow-fleshed genotypes partially shifted their carbon allocation away from starch accumulation and favored the accumulation of *myo*-inositol, raffinose, and the biosynthesis of building blocks for pectin and hemicellulose. Finally, cell wall component measurements revealed that yellow cultivars exhibit a significant increase of nearly all cell wall components measured, supporting the conclusion that yellow-fleshed cassava cultivars divert more carbon for cell wall synthesis at the expense of their starch content.

RESULTS AND DISCUSSION

Comparative harvest data analysis confirmed a negative correlation between starch and carotenoid content in 49 African *Manihot esculenta* genotypes

A breeding panel of 49 African cassava genotypes from the International Institute of Tropical Agriculture (IITA) was grown under field conditions for 12 months in Ibadan, Nigeria. Phenotypic data recorded during the harvest included starch, dry matter, and carotenoid content of the storage roots. As depicted in Figure 1A, starch content in the samples under investigation varied from 9 to 34%, depending on the genotype. Carotenoid content in cassava roots was indirectly estimated based on root yellowness intensity, as indicated by the CIELAB Chromameter *b** value (Figure 1B). This method does not provide direct quantification of carotenoid levels but rather offers a

© 2024 The Author(s).

1365313x, 2024, 4, Downloaded from https://onlinelibrary.wiley.com/doi/10.1111/tpj.16909 by Nigeria Hinari NPL, Wiley Online Library on [02/12/2024]. See the Terms and Conditions (https://onlinelibrary.wiley.com/terms-and-conditions) on Wiley Online Library for rules of use; OA articles are governed by the applicable Creative Commons License

relative assessment based on color intensity. The *b** value, representing yellowness, ranged from 14 to 48. This color-based estimation is grounded in the known strong correlation between root yellowness and carotenoid content in cassava (Sánchez et al., 2014). We could not detect any significant correlation between root fresh weight and dry matter or starch content (Figure 1C). Chávez et al. (2005) also reported no significant correlation between starch content and root fresh weight across multiple cassava genotypes. However, both negative and positive correlations between these traits were reported (Adeniji et al., 2011; Ntawuruhunga & Dixon, 2010). The lack of a consistent correlation between starch content and root fresh weight in cassava highlights the complexity of the factors influencing root yield and starch accumulation in this crop and suggests that the relationship between these two traits may be influenced by multiple interacting factors. This includes genetic factors, environmental conditions, and developmental processes. However, a positive correlation between starch content and dry matter content ($r = 0.9$, $P \leq 0.05$), as well as a negative correlation ($r = -0.6$, $P \leq 0.05$) for starch and carotenoid content, could be identified (Figure 1C–E). This shows that while high-carotenoid varieties still accumulate starch in roots, a drop in starch levels occurs if carotenoid content exceeds a certain amount. Besides that, it also demonstrates that yellow varieties show high variance concerning the accumulation of starch in the storage roots (Figure 1).

Segregation of white and yellow genotypes based on metabolite profiling

Storage root samples from the 49 unique African cassava genotypes included in the phenotypic profiling were subjected to GC–MS analysis, and 50 metabolites were measured (Tables S1 and S2). Absolute metabolite values were *z*-score transformed and used to identify metabolites showing significantly different abundance between white and yellow genotypes, or were correlated to starch in white or yellow varieties, respectively. Overall, 16 metabolites exhibited a significantly different abundance between white and yellow genotypes (Figure 2). Notably, sucrose, fucose, raffinose, and xylose, among other metabolites such as *myo*-inositol, malate, fumarate, tyrosine, glutamine, and β-alanine, exhibited statistically significant decrease in abundance in white genotypes compared to yellow genotypes (Figure 2). Among the metabolites examined, only three—nicotinic acid, 4-hydroxy-*trans*-proline, and glutamate—exhibited significantly higher abundance in the white genotypes compared to the yellow genotypes. When analyzing the correlations between starch content and all metabolites showing significantly different abundance between the two genotype groups, only 4-hydroxy--*trans*-proline revealed a significant positive correlation with starch in the yellow genotypes. The remaining metabolites consistently showed negative correlations with starch content in both white and yellow genotypes (Figure 2).

The differences in metabolite abundance, particularly the higher levels of sucrose, glucose, and fructose, suggest that the reduced starch formation in yellow genotypes is unlikely resulting from a limited carbon source supply. Sucrose, fructose, and glucose were also negatively correlated with starch in both white and yellow genotypes, indicating a differentiation in carbon allocation rather than reduced photosynthetic performance in the yellow varieties. This accumulation of sugars in the storage root of low-dry-matter genotypes has also been reported in a smaller subset of the same African cassava genotype panel by Lamm et al. (2023), recently.

Segregation into white and yellow genotypes based on *PSY2* sequence

The storage root samples from the 49 unique African cassava genotypes used for metabolite profiling were also subjected to RNA sequencing using the protocol of the Illumina NovaSeq6000 system (PE150 + 150; Novogene, Cambridge, UK). After removing adapters and performing quality trimming (Q35), an average of 21 million paired-end reads per sample were retained. Sequence alignment to the reference genome yielded an average mapping efficiency of 91% for uniquely mapped reads and 4% for multi-mapped reads.

Sequence analyses of the *PSY*2 reads showed that the genotype groups carry different alleles for that locus. All varieties characterized as "yellow" showed the same A to C substitution in the *PSY*2 transcript (Chromosome 1, Position 31960252 in *Manihot esculenta* v8.1 reference genome) as described by Welsch et al. (2010). All white genotypes displayed the null version of this allele. This not only supports the distinction between white and yellow genotypes but also demonstrates that carotenoid biosynthesis in yellow-fleshed *Manihot esculenta* storage roots is primarily driven by the allelic differences in *PSY*2 (Table S3). However, the regulations driving differential starch accumulation in the yellow genotypes remain unclear.

Transcriptional separation and correlation analysis for white and yellow varieties

All uniquely mapped reads were additionally subjected to variance-stabilizing transformation and depth filtration (⩾10), identifying approximately 20 000 genes as being expressed in at least one of the genotype groups. Principal component analysis (PCA) of all expressed genes revealed distinct clustering patterns that distinguish white from yellow genotypes along PC1. Notably, the lack of overlap between the clusters for white and yellow genotypes underscores a transcriptional divergence that accounts for 61% of the observed variance in PC1 (Figure 3A). A

© 2024 The Author(s).

1365313x, 2024, 4, Downloaded from https://onlinelibrary.wiley.com/doi/10.1111/tpj.16909 by Nigeria Hinari NPL, Wiley Online Library on [02/12/2024]. See the Terms and Conditions (https://onlinelibrary.wiley.com/terms-and-conditions) on Wiley Online Library for rules of use; OA articles are governed by the applicable Creative Commons License

follow-up differential expression analysis uncovered a total of 472 differentially expressed genes (DEGs) between white and yellow genotypes with an even distribution across all chromosomes (Figure 3B,C; Figure S1). Of these, 71 DEGs were highly expressed in white varieties, and 401 DEGs were highly expressed in yellow varieties (Figure 3B;

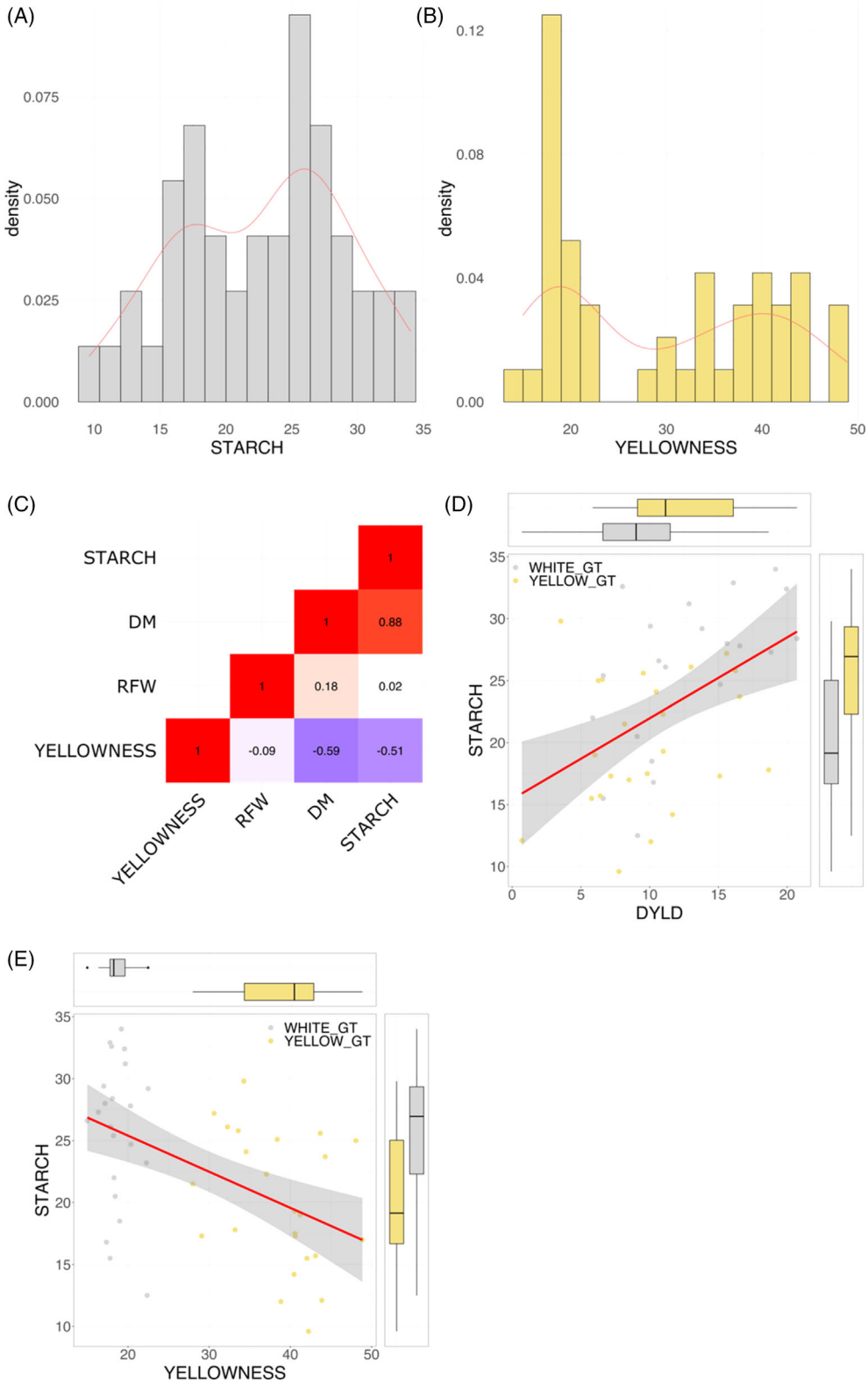

© 2024 The Author(s).

1365313x, 2024, 4, Downloaded from https://onlinelibrary.wiley.com/doi/10.1111/tpj.16909 by Nigeria Hinari NPL, Wiley Online Library on [02/12/2024]. See the Terms and Conditions (https://onlinelibrary.wiley.com/terms-and-conditions) on Wiley Online Library for rules of use; OA articles are governed by the applicable Creative Commons License

Figure 1. Phenotype and metabolite data representation.
(A, B) Density plot depicting the distribution of all genotypes under investigation according to their starch or carotenoid content.
(C) Heatmap depicting the correlation among starch, dry matter (DM), yellowness, and root fresh weight (RFW). Red color indicates a positive and blue colors a negative correlation. The filling of the heatmap boxes indicates the correlation strength.
(D, E) Connection between starch content (percentage) and dry yield (DYLD) or carotenoid content (yellowness; represented by chromameter *b** value) and distribution across all genotypes under investigation. Yellow color refers to low-starch/high-carotenoid genotypes, whereas gray represents high-starch/low-carotenoid genotypes. Black line with the surrounding gray bar depicts the linear relationship between the variables with its corresponding 0.95 confidence interval.

Table S4). However, similar to the results of Olayide et al. (2023), almost no significant difference in the expression of genes annotated as part of the carotenoid biosynthesis pathway could be detected between white and yellow genotypes. This aligns with the finding that the C to A substitution in *PSY2* increases its enzyme activity (Welsch et al., 2010) and suggests that differences in carotenoid biosynthesis in the yellow-fleshed cassava storage roots analyzed here are primarily driven by the allelic differences in *PSY*2. Only *DXS*, which catalyzes the first step in the MEP pathway, was detected with a significantly higher abundance in yellow genotypes compared to white genotypes (Figure 4; Table 1). In *Solanum lycopersicum* and *Arabidopsis thaliana*, an enhanced enzyme activity of PSY was associated with a post-transcriptional accumulation of DXS (Fraser et al., 2007; Rodríguez-Villalón et al., 2009). Studies in Arabidopsis have shown that DXS is the enzyme with the highest flux control through the carotenoid biosynthesis pathway (Wright et al., 2014). This could explain the higher transcript levels of *DXS* in yellow cassava storage roots, although the reported allele-specific enzyme activity increase of *PSY2* (Welsch et al., 2010) likely has a bigger effect on carotenoid levels.

Our analyses not only revealed a negative correlation between starch and carotenoid content but we also showed that yellow cultivars have different starch contents despite hetero- or homozygosity for the $C_{572}A$ nucleotide substitution in *PSY2* and the resulting characterization as yellow fleshed. This raises the question of how carbon is allocated within the yellow genotypes and how the variance in starch accumulation, despite the carotenoid levels, can be explained and compared to the mechanisms in white genotypes.

Considering the negative correlation between starch and carotenoid content, direct analyses of gene expression and starch content without accounting for carotenoid levels could lead to misleading conclusions. Specifically, gene expressions associated with starch metabolism might inadvertently reflect the influence of the correlation between starch and carotenoid levels. To accurately capture the true relationships between gene expression and starch content solely, we performed a partial correlation analysis. This statistical approach allowed us to isolate the relationship between gene expression and starch content and to filter out potential (direct or indirect) influences from the variety's carotenoid content. Therefore, high-quality, depth-filtered (≥10) reads that underwent variance-stabilizing transformation were used to identify genes with expression profiles significantly correlated to starch content. By performing partial correlation analysis separately for white and yellow genotypes, the analysis now accounts for the variety's carotenoid level as a confounding effect. As shown in Table 2, white genotypes displayed an overall higher number of genes significantly correlated with starch content. Additionally, a proportionally higher number of these genes showed positive correlation to starch (see Table S5). Functional enrichment analysis for the white genotypes revealed that the expression of positively correlated genes was enriched in the "Protein processing in endoplasmatic reticulum," "Nucleotide metabolism," "Pyrimidine metabolism," and "Thiamine metabolism" according to the Kyoto Encyclopedia of Genes and Genomes (KEGG). In contrast, yellow varieties showed enrichment in genes related to "Starch and sucrose metabolism," "Amino sugar and nucleotide sugar metabolism," "Biosynthesis of nucleotide sugars," and others. For genes negatively correlated to starch content within the white and yellow genotypes, enrichment was observed in genes annotated as part of "Ribosomes," "D-Amino acid metabolism" and "Ribosome biogenesis in eukaryotes" (see Figure S2).

White and yellow genotypes show positive correlation between genes involved in starch biosynthesis

Photoassimilates produced in cassava source leaves are converted into high-sucrose levels and enter the phloem in a largely passive, symplasmic manner (Rüscher et al., 2024). Sucrose transport to the existing xylem parenchyma of storage roots via the phloem tissue and vascular rays also happens symplasmically (Mehdi et al., 2019). As depicted in Figure 4, incoming sucrose can then be cleaved into glucose and fructose by cytosolic invertases (cINV) and further phosphorylated by hexo- or fructokinases (HXK; FRK) to form glucose- or fructose-6-phosphate (G6P; F6P). Glucose-6-phosphate isomerase can act as an intermediate catalyst for the conversion of F6P to G6P. However, cassava mainly utilizes sucrose synthase (SUS) in its storage roots to cleave incoming sucrose into UDP-glucose and fructose

© 2024 The Author(s).

1365313x, 2024, 4, Downloaded from https://onlinelibrary.wiley.com/doi/10.1111/tpj.16909 by Nigeria Hinari NPL, Wiley Online Library on [02/12/2024]. See the Terms and Conditions (https://onlinelibrary.wiley.com/terms-and-conditions) on Wiley Online Library for rules of use; OA articles are governed by the applicable Creative Commons License

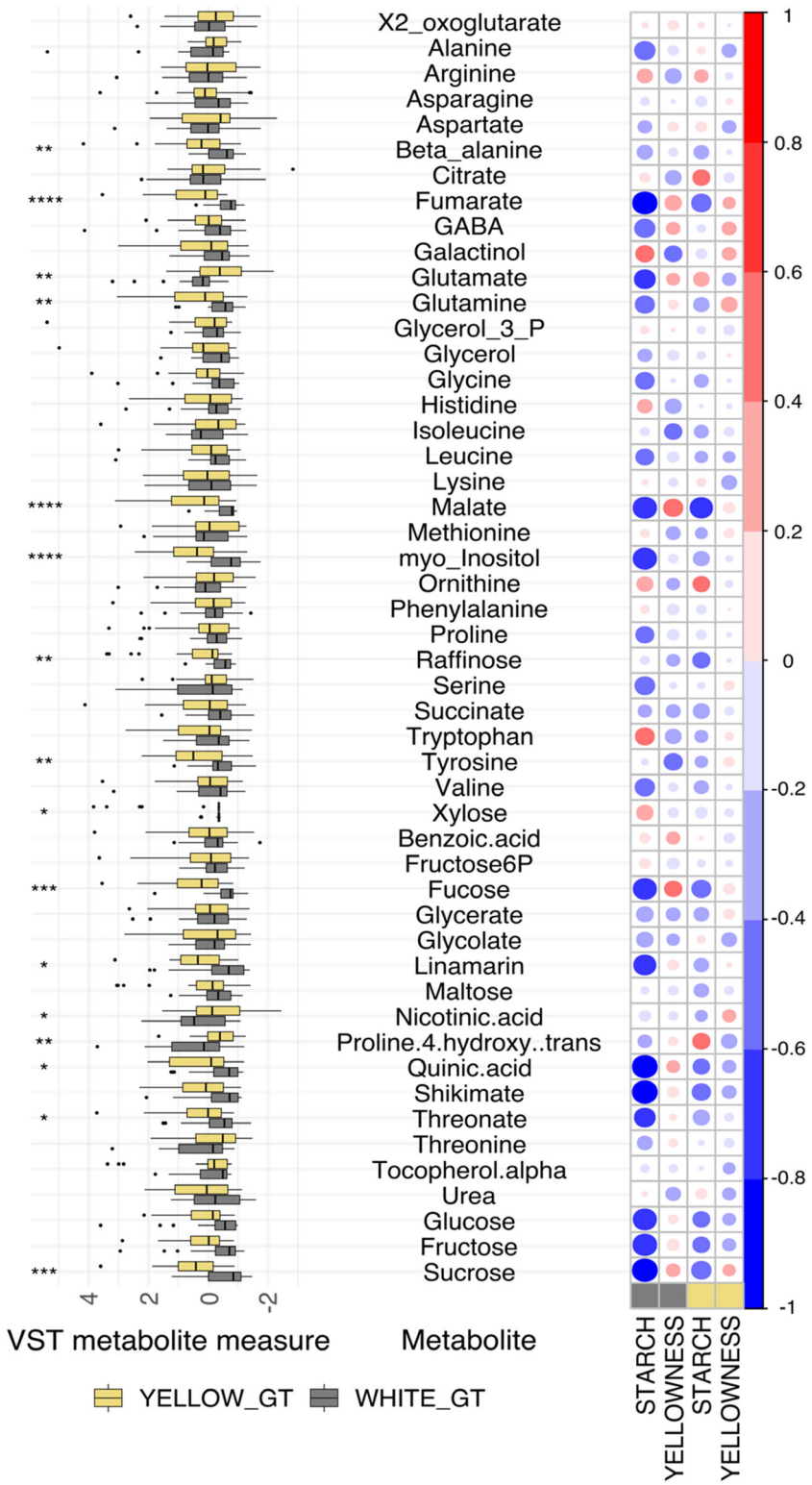

Figure 2. Representation of metabolite information, differences between examined genotype groups, and their correlation to starch and carotenoid content. The left side represents all measured metabolites and their difference in abundance between white and yellow genotypes. Yellow color refers to low-starch/high-carotenoid genotypes, whereas gray represents high-starch/low-carotenoid genotypes. The right side depicts correlation analysis of all measured metabolites to starch and yellowness. Boxes at the bottom represent low-starch/high-carotenoid (yellow) and high-starch/low-carotenoid (gray) genotypes. Red colors indicate a positive, and blue colors a negative correlation. The circle sizes display the correlation strength. Asterisks (*; ** and ***) refer to the significance level of the corresponding *P*-value (≤0.05; ≤0.01; and ≤0.001).

© 2024 The Author(s).

1365313x, 2024, 4, Downloaded from https://onlinelibrary.wiley.com/doi/10.1111/tpj.16909 by Nigeria Hinari NPL, Wiley Online Library on [02/12/2024]. See the Terms and Conditions (https://onlinelibrary.wiley.com/terms-and-conditions) on Wiley Online Library for rules of use; OA articles are governed by the applicable Creative Commons License

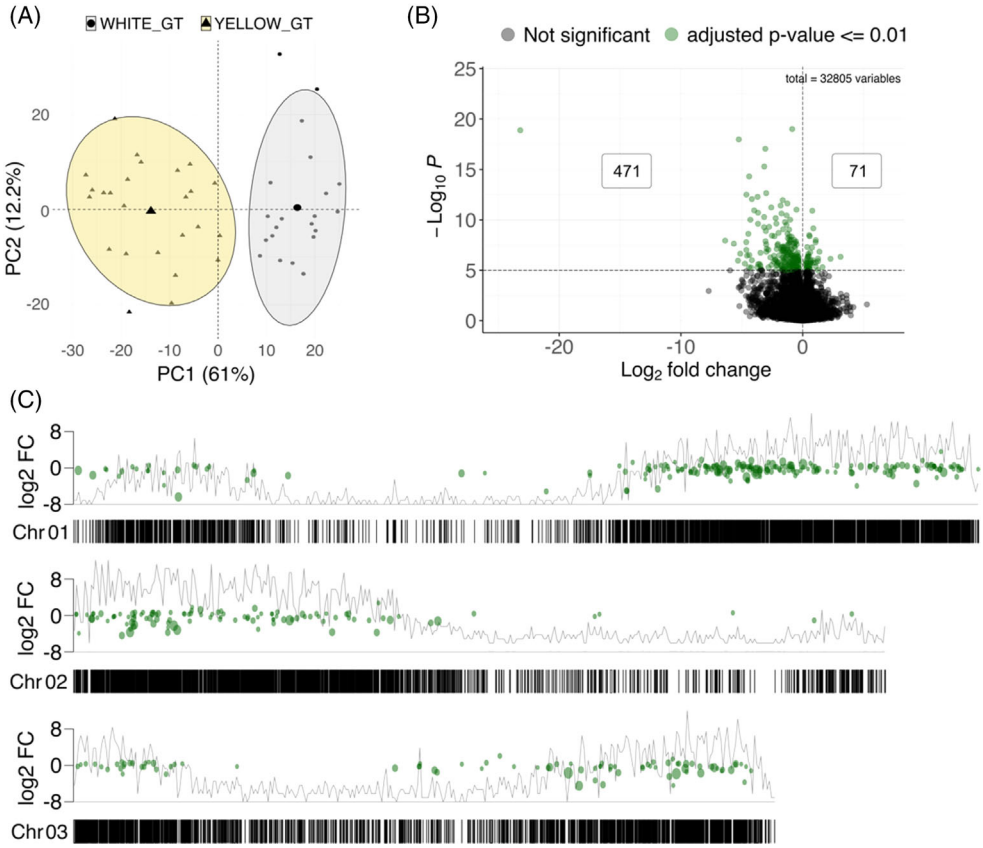

Figure 3. Representation of transcriptional information and differences between examined genotype groups.
(A) Principal component analysis representing PC1 and PC2 for read count-filtered transcriptomic data. Small triangles and yellow circle label yellow genotypes, whereas the gray circle and small black dots represent white genotypes. Enlarged triangle and black dot highlight the center of the corresponding genotype distribution in PC1 and PC2 dimensions.
(B) Volcano plot representing all genes between white and yellow genotypes. Black dots depict genes with no significant difference between white and yellow genotypes. Green dots refer to genes that match the significance threshold. Positive Log2FC values refer to a higher expression in white, whereas negative values represent a higher expression in yellow genotypes.
(C) Chromosomal distribution of all detected significantly differential expressed genes between white and yellow genotypes. Black bars at the bottom depict the localization of genes on the respective chromosome. The line in the background represents the number of transcripts for that position. Green dots refer to the significant differentially expressed genes for that chromosome. *Y*-axis and equivalent height of green dots indicate changes in gene expression comparing white with yellow genotypes—positive values refer to a higher expression in white, whereas negative values represent a higher expression in yellow genotypes. For conciseness, only the first three chromosomes are shown. For representation of all chromosomes, see Figure S1.

(Mehdi et al., 2019). Fructose is phosphorylated by FRK, while UDP-glucose phyrophosphorylases (UGPases) and phosphoglucomutases (PGMs) catalyze the reaction of UDP-glucose to G1P and then to G6P, respectively. When analyzing these genes for their expression patterns between white and yellow genotypes and their correlation to starch, while accounting for carotenoid levels as a confounding factor (Figure 4; Table 3; Tables S5 and S6), only one of three *cINV*s was detected as being higher expressed in white compared to yellow genotypes. The remaining two isoforms did not show differential expression between white and yellow genotypes. Additionally, none of them exhibited an expression pattern correlated with starch in either genotype group, even though all *cINV*s annotated transcripts were expressed in both genotype groups. *SUS* also did not show significant differential expression between the genotype groups, however, one isoform was positively correlated to starch in white genotypes. Furthermore, six of nine *SUS* transcripts showed similar expression in both genotype groups. One *UGPase* isoform was found to have significantly higher abundance in yellow genotypes, whereas a different isoform was positively correlated to starch in white genotypes. The two cytosolic isoforms of *PGM* did not show any significant correlation to starch or differential expression between the genotype groups, although being expressed in both white and yellow genotypes (Figure 4; Table 3; Tables S5 and S6).

Despite the lack of differential expression for sucrose-cleaving enzyme genes, significantly higher sucrose content and a trend towards higher glucose and

© 2024 The Author(s).

1365313x, 2024, 4, Downloaded from https://onlinelibrary.wiley.com/doi/10.1111/tpj.16909 by Nigeria Hinari NPL, Wiley Online Library on [02/12/2024]. See the Terms and Conditions (https://onlinelibrary.wiley.com/terms-and-conditions) on Wiley Online Library for rules of use; OA articles are governed by the applicable Creative Commons License

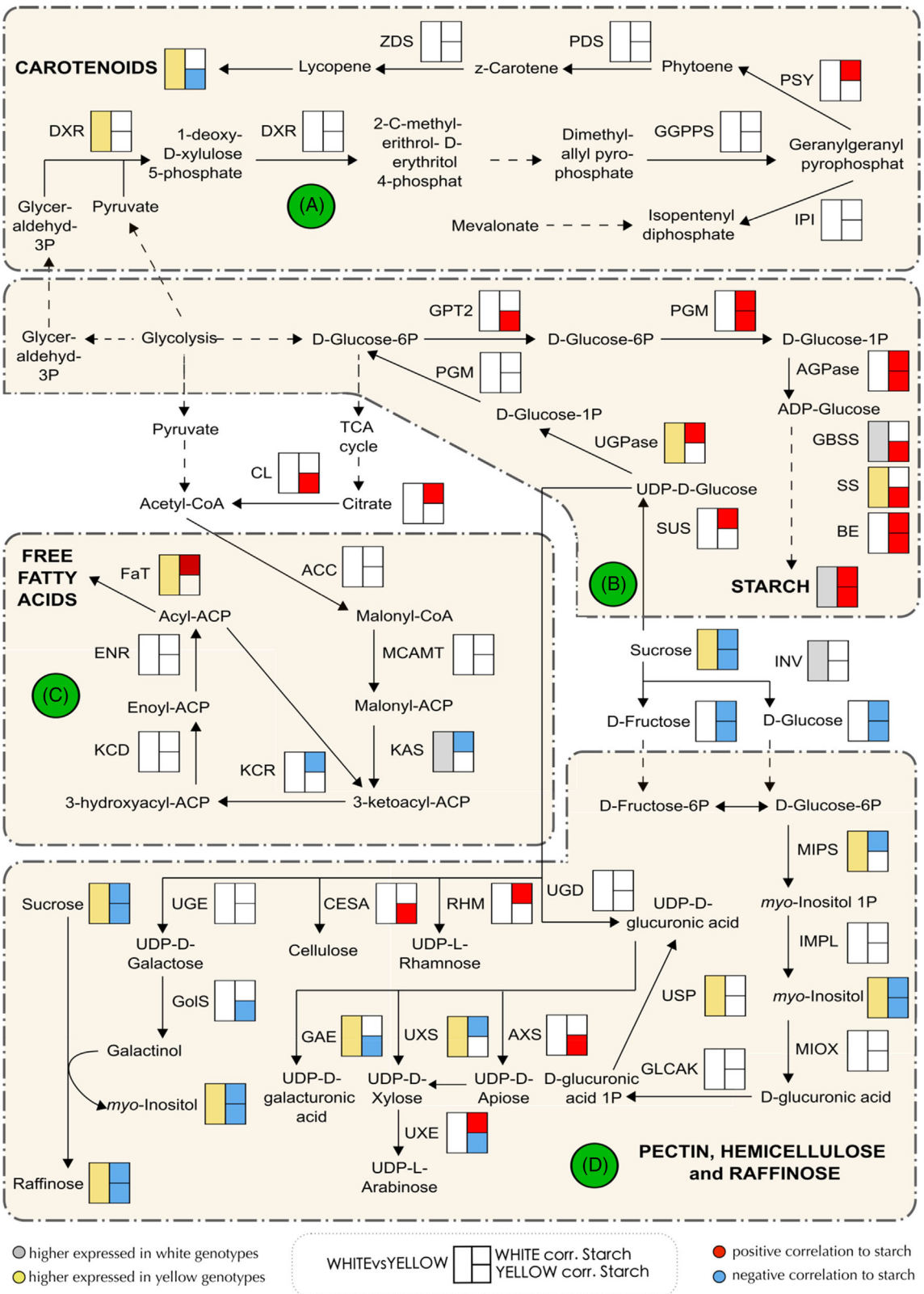

© 2024 The Author(s).

1365313x, 2024, 4, Downloaded from https://onlinelibrary.wiley.com/doi/10.1111/tpj.16909 by Nigeria Hinari NPL, Wiley Online Library on [02/12/2024]. See the Terms and Conditions (https://onlinelibrary.wiley.com/terms-and-conditions) on Wiley Online Library for rules of use; OA articles are governed by the applicable Creative Commons License

Figure 4. Gene expression patterns, correlation to starch, and metabolite abundance.
Model depicting the observed differences in gene (at least one for the corresponding group) or metabolite abundance between white and yellow genotypes and correlation to starch in either white or yellow genotypes for (A) carotenoid biosynthesis, (B) sucrose breakdown and starch synthesis, (C) de novo fatty acid synthesis, and (D) synthesis of cell wall components and raffinose. Bigger left boxes shown beside the gene (*A. thaliana* homolog) or metabolite are filled gray if significantly higher abundant in white genotypes or yellow if significantly higher in yellow genotypes. Smaller boxes on the right show the significant correlation to starch with the upper box representing the correlation to starch in white genotypes and the lower for yellow genotypes. Red color indicates a positive correlation and blue a negative. Dashed lines refer to a non-direct synthesis path. Gene identifier, isoform, corresponding *A. thaliana* homolog, correlation coefficients, *P*-value, and general abundance for all shown genes and metabolites are additionally provided in Data S1. For detailed functional pathway description, see main text.

Table 1 Enzymes related to carotenoid biosynthesis and identified as correlated to starch or significantly differentially expressed between white and yellow genotypes

Enzyme	Isoform	Locus identifier	Corr. coeff WHITE	Corr. coeff YELLOW	Expression sign. higher in
1-Deoxy-D-xylulose 5-phosphate synthase	DXS1	Manes.15G018800	n.s.	n.s.	YELLOW
	DXS1	Manes.13G101600	n.s.	n.s.	YELLOW
4-Cytidine-5′-diphospho-2-C-methyl-D-erythritol kinase	CMK	Manes.01G176400	n.s.	−0.45	n.s.
Phytoene synthase	PSY	Manes.02G081700	0.70	n.s.	n.s.

Table 2 Number of genes correlated to starch and separated for white and yellow genotypes

Number of genes correlated to starch	White genotypes	Yellow genotypes
Positive correlation	1024	665
Negative correlation	942	736
∑	1966	1401

fructose levels (not significant) were observed in the yellow cultivars. This could reflect a lower flux through the SUS-mediated metabolic pathway and a preference for the cINV metabolic pathway in the yellow cultivars studied here. Similar observations were also made by Lamm et al. (2023), who investigated metabolic and proteomic differences in eight *Manihot esculenta* genotypes of the same genotype panel. On protein level, the authors previously found indications for a shift from cINV- to SUS-mediated sucrose cleavage and an increased allocation of sugars to the amyloplasts in high-dry-matter genotypes.

G6P can enter the amyloplast via the glucose-6-phosphate translocator (GPT) and is converted back to G1P by PGMp. G1P is subsequently converted to ADP glucose, catalyzed by ADP glucose pyrophosphorylase (AGPase), providing the building blocks for starch. One of two *GPT2* isoforms was identified as DEG between white and yellow genotypes, with higher expression in white genotypes. However, both isoforms were detected as positively correlated to starch only in the yellow genotypes. This specific difference between white and yellow genotypes suggests that the uptake of G6P into the amyloplasts might be an important point of metabolic divergence between white and yellow genotypes. The importance of carbon and energy uptake into amyloplasts for starch synthesis was previously demonstrated in potato tubers (Jonik et al., 2012; Zhang et al., 2008). The two plastidic *PGM* isoforms showed the same expression levels between the genotype groups. One with positive correlation to starch in both groups, the second with positive correlation only in yellow genotypes. Four *AGPase* subunits were identified with no differential expression comparing white and yellow genotypes. However, for both genotype groups, a positive correlation between the expression of *AGPase* and starch could be observed, although a different isoform of *AGPase* significantly correlated in each genotype group.

Among many other proteins, granule-bound starch synthase (GBSS), starch synthase (SS), and starch branching enzyme (BE) produce amylopectin and amylose, the two main components of storage starch (Figueroa et al., 2022; Munyikwa et al., 1997). Although it was shown that debranching enzymes (DBE) are not strictly necessary for starch formation (Zeeman et al., 2010), they can also contribute to amylopectin synthesis. One *GBSS* isoform showed a higher abundance in white genotypes and a positive correlation to starch in the yellow genotypes examined here. One *SS* and two *BE* isoforms exhibited a positive correlation to starch in yellow genotypes, with one *SS* isoform also showing a higher expression in yellow genotypes (Figure 4; Table 3; Tables S5 and S6).

Overall, both genotype groups share similar gene expression and correlation patterns for genes known to be involved in sucrose breakdown and starch biosynthesis.

White and yellow genotypes show only minor differences in expression of genes involved in *de novo* fatty acid biosynthesis and their correlation to starch

Increased carotenoid levels in cassava co-occur not only with a decrease in starch content but were also shown to

© 2024 The Author(s).

1365313x, 2024, 4, Downloaded from https://onlinelibrary.wiley.com/doi/10.1111/tpj.16909 by Nigeria Hinari NPL, Wiley Online Library on [02/12/2024]. See the Terms and Conditions (https://onlinelibrary.wiley.com/terms-and-conditions) on Wiley Online Library for rules of use; OA articles are governed by the applicable Creative Commons License

Table 3 Enzymes related to starch biosynthesis and identified as correlated to starch or significantly differentially expressed between white and yellow genotypes

Enzyme	Isoform	Locus identifier	Corr. coeff WHITE	Corr. coeff YELLOW	Expression sign. higher in
ADP glucose pyrophosphorylase	ADG1	Manes.13G058900	0.57	n.s.	n.s.
	ADG1	Manes.12G067900	n.s.	0.52	n.s.
Branching enzyme	BE2	Manes.05G073400	0.6	0.51	n.s.
	BE3	Manes.05G133800	n.s.	0.58	n.s.
Cytosolic invertase	CINV2	Manes.18G103000	n.s.	n.s.	WHITE
Debranching enzyme	DBE1	Manes.05G073400	0.6	0.51	n.s.
	DBR1	Manes.03G006700	n.s.	n.s.	WHITE
Fructokinase	FRK4	Manes.11G121800	n.s.	0.47	n.s.
Glucose 6-phosphate/phosphate translocator	GPT2	Manes.16G010700	n.s.	0.69	WHITE
	GPT2	Manes.17G036800	n.s.	0.47	n.s.
Granule-bound starch synthase	GBSS1	Manes.02G001000	n.s.	0.67	WHITE
Hexokinase	HXK1	Manes.16G109200	−0.49	n.s.	n.s.
	HXK3	Manes.18G014000	n.s.	n.s.	YELLOW
Phosphoglucomutase	PGM	Manes.14G031100	0.52	0.57	n.s.
	PGM	Manes.06G141300	n.s.	0.44	n.s.
Starch-branching enzyme	SBE2.2	Manes.08G022400	n.s.	0.63	n.s.
Starch synthase	SS2	Manes.02G046733	n.s.	0.52	n.s.
	SS2	Manes.01G091700	n.s.	n.s.	YELLOW
Sucrose synthase	SUS6	Manes.14G107800	0.6	n.s.	n.s.
UDP-glucose pyrophosphorylase	UGP2	Manes.02G080600	0.62	n.s.	n.s.
	UGP2	Manes.01G123000	n.s.	n.s.	YELLOW

Table 4 Enzymes related to the *de novo* fatty acid biosynthesis and identified as correlated to starch or significantly differentially expressed between white and yellow genotypes

Enzyme	Isoform	Locus identifier	Corr. coeff WHITE	Corr. coeff YELLOW	Expression sign. higher in
3-Ketoacyl-ACP synthase	KASI	Manes.02G007650	n.s.	n.s.	WHITE
	KAS II	Manes.03G043700	−0.51	n.s.	WHITE
Beta-ketoacyl reductase	KCR1	Manes.12G018500	−0.51	n.s.	n.s.
Fatty acyl-ACP thioesterases	FATB	Manes.16G064400	n.s.	n.s.	YELLOW
	FATB	Manes.11G051800	0.56	n.s.	n.s.

coincide with an increase in fatty acid concentrations (Beyene et al., 2018), which indicates competition for carbon skeletons between *de novo* fatty acid and starch synthesis due to redirection of carbon resources.

To address whether there is a transcriptional or metabolic basis for these observations in the genotypes analyzed here, we investigated the gene expression and metabolite abundance known to be involved in *de novo* fatty acid biosynthesis (Guschina & Harwood, 2007; Harwood, 1996; Figure 4; Table 4; Tables S5 and S6). White and yellow genotypes only exhibited small alterations in gene expression associated with *de novo* fatty acid synthesis and correlations to starch were almost exclusively negative. As depicted in Figure 4 and Table 4, one *3-ketoacyl-ACP synthase* (*KASII*) isoform was detected to be negatively correlated to starch and significantly higher abundant in white genotypes. *KASI* also found higher expression in white genotypes but did not show any correlation to starch. One *ß-ketoacetyl-CoA reductase* (*KCR*) isoform was identified with a negative correlation to starch in white genotypes. Additionally, one isoform of fatty acyl-ACP thioesterase (*FaTB*) exhibited a positive correlation to starch, while a second one was higher expressed in the yellow compared to the white genotypes. None of the other genes involved in *de novo* fatty acid synthesis showed significant differential expression between white and yellow genotypes, even though almost all of them were expressed in both genotype groups (Figure 4; Table 4; Tables S5 and S6).

Acetyl-CoA could represent a point of metabolic convergence between starch and fatty acid synthesis. Acetyl-CoA can be synthesized from free acetate via the action of acetyl-CoA synthetase (ACS), from pyruvate by the reaction catalyzed by pyruvate dehydrogenase complex (PDC) in the plastid or mitochondria, and from free acetate through the action of a plastidic carnitine acetyltransferase, which transfers acetate from acetyl-carnitine to CoA, or through

© 2024 The Author(s).

1365313x, 2024, 4, Downloaded from https://onlinelibrary.wiley.com/doi/10.1111/tpj.16909 by Nigeria Hinari NPL, Wiley Online Library on [02/12/2024]. See the Terms and Conditions (https://onlinelibrary.wiley.com/terms-and-conditions) on Wiley Online Library for rules of use; OA articles are governed by the applicable Creative Commons License

Table 5 Enzymes related to the *myo*-inositol, raffinose, and cell wall biosynthesis and identified as correlated to starch or significantly differentially expressed between white and yellow genotypes

Enzyme	Isoform	Locus identifier	Corr. coeff WHITE	Corr. coeff YELLOW	Expression sign. higher in
Cellulose synthase	CESA1	Manes.16G120400	n.s.	0.49	n.s.
	CESA6	Manes.12G146600	n.s.	0.6	n.s.
	CESA6	Manes.12G148100	n.s.	0.48	n.s.
Galactinol synthase	GolS1	Manes.01G231500	n.s.	−0.46	n.s.
Myo-inositol-1-phosphate synthase	MIPS2	Manes.13G091100	n.s.	−0.44	YELLOW
Myo-inositol polyphosphate 5-phosphatase	5PTASE2	Manes.15G174000	0.52	n.s.	n.s.
Raffinose synthase	RS2	Manes.14G057700	n.s.	−0.42	n.s.
	RS5	Manes.17G115500	n.s.	n.s.	YELLOW

the ATP-citrate lyase (ACL) (Ke et al., 2000; Rawsthorne, 2002). However, we could not detect differential expression between the white and yellow genotypes, nor a significant correlation to starch of acetyl-CoA-synthesizing genes. Genes involved in glycolysis or the TCA cycle were generally not differentially expressed either. However, one isoform of *phosphoglycerate kinase* (*PGK*3) did indeed show significantly higher abundance in white genotypes and a positive correlation to starch in yellow varieties. Additionally, two *E1 alpha subunits of pyruvate dehydrogenase complexes* (*PDCs*) genes were significantly higher expressed in yellow genotypes, with one of them positively correlated to starch in white varieties (Tables S4–S6).

Based on these results, the transcriptome data and gene expression patterns in the cassava genotypes studied do not convincingly support a clear shift from starch to fatty acid synthesis in the yellow varieties. While lower-starch levels and higher-carotenoid concentrations were observed alongside increased fatty acid concentrations (Beyene et al., 2018), the transcriptional and metabolic evidence suggests that starch and fatty acid synthesis may not necessarily directly compete with each other in the varieties analyzed here. This observation aligns with previous research on other plant species. For example, Klaus et al. (2004) analyzed potato lines with reduced activities of AGPase or plastidial PGM to test redirection of carbon to fatty acid synthesis and revealed that the block in the limiting steps in starch synthesis did not result in a redirection of carbon into lipid synthesis in *Solanum tuberosum* L. plants. Overall, despite some alterations in the expression of particular genes related to *de novo* fatty acid biosynthesis, the lack of significant differential expression for most of these genes implies a complex metabolic regulation but does not point toward a clear and convincing direct trade-off.

Transcript and metabolite levels highlight significant higher abundance of genes and metabolites associated with *myo*-inositol, raffinose, and cell wall biosynthesis in yellow genotypes

Myo-inositol in plants serves many diverse functions. To name just a few, it is a key metabolite for signaling and cellular communication, a precursor for phosphate storage (in form of phytate), and is needed for cell wall biosynthesis and the production of stress-related oligosaccharides like raffinose or stachyose.

Myo-inositol can be synthesized *de novo* from G6P by converting it to *myo*-inositol-1-phosphate by the action of *myo*-inositol-1-phosphate synthase (MIPS) in the rate-limiting step of inositol biosynthesis and to *myo*-inositol by the reaction catalyzed by *myo*-inositol phosphatases (IMP). Oligosaccharides, such as raffinose and stachyose, are formed from *myo*-inositol by the conversion from *myo*-inositol and UDP-D-glucose to galactinol via galactinol synthases (GolS). Raffinose synthases (RS) then catalyze the transfer of the galactosyl unit from galactinol to sucrose, yielding raffinose. Stachyose synthases (STS) further transfer the galactosyl moiety from galactinol to galactose to produce stachyose (Loewus & Loewus, 1983; Loewus & Murthy, 2000).

The yellow genotypes analyzed here exhibit higher abundance of all measured metabolites involved in *myo*-inositol and raffinose synthesis. As depicted in Figures 2 and 4, sucrose, *myo*-inositol, and raffinose were detected with significantly higher abundance in yellow compared to white genotypes. The elevated levels of *myo*-inositol might additionally trigger raffinose and stachyose synthesis in the yellow-fleshed cassava varieties. *RS1* was indeed detected with a significantly higher expression in yellow compared to white genotypes (Figure 4; Table 5; Tables S4–S6). Furthermore, *GolS1*, *RS1*, and *RS5* were identified with a significant negative correlation to starch in the yellow genotypes. Stachyose was not measured in the metabolite data analyzed here but *STS* was not found to be differentially expressed between white and yellow genotypes nor to show a correlation to starch in either of the genotype groups (Figure 4; Table 5; Tables S4–S6). Raffinose family oligosaccharides (RFOs) are known to be responsible for a wide variety of functions in both plants and the human diet. In recent years, RFOs have been heavily studied and identified to be involved in various stress responses in crops (Yan et al., 2022). For example, previous studies observed raffinose levels to be higher in

© 2024 The Author(s).

1365313x, 2024, 4, Downloaded from https://onlinelibrary.wiley.com/doi/10.1111/tpj.16909 by Nigeria Hinari NPL, Wiley Online Library on [02/12/2024]. See the Terms and Conditions (https://onlinelibrary.wiley.com/terms-and-conditions) on Wiley Online Library for rules of use; OA articles are governed by the applicable Creative Commons License

plants showing increased cold tolerance in *A. thaliana*, rice, and sugar beet (Keller et al., 2021; Klotke et al., 2004; Morsy et al., 2007). Furthermore, RFOs are thought to be important for plant tolerance against heat stress, oxidative stress, drought, salt, or biotic stresses (Yan et al., 2022). African *cassava* varieties are subjected to multiple seasonal stressors like heat and drought during their growth period. Increased production of galactinol and raffinose through increased metabolic flux toward *myo*-inositol suggests that yellow-fleshed cassava genotypes might use it as a protective mechanism for the stress they are exposed to. Even though we could detect *GolS1*, *RS1*, and *RS5* with a negative correlation to starch and a higher abundance in yellow genotypes, we can only hypothesize that the yellow genotypes might be better prepared for certain biotic or abiotic stresses. Lastly, it is worth noting that some characteristics of RFOs need to be considered for human consumption. Despite their reported potential health benefits, such as anti-allergic, anti-obesity, and anti-diabetic potentials (Kanwal et al., 2023), RFOs are considered anti-nutritional factors. The human digestive system lacks the capacity to digest RFOs in the intestines, leading to their fermentation by gut microbiota. This fermentation process can cause intestinal symptoms like flatulence, abdominal cramps, diarrhea, and nausea. It is also important to recognize that these symptoms act as a barrier to RFO consumption in humans (Elango et al., 2022; Sanyal et al., 2023). Moreover, an increased proportion of RFOs in crops intended for human consumption may reduce the availability of metabolizable carbohydrates that serve as an energy source for humans. Consequently, the presence of RFOs in crops should be carefully managed to maintain an optimal balance between their benefits for crop cultivation and potential drawbacks for human consumers.

In cell wall biosynthesis, UDP-glucuronic acid is synthesized via two different pathways. The primary pathway involves the direct conversion of UDP-glucose to UDP-glucuronic acid by UDP-glucose dehydrogenase (UGD). In the secondary pathway, *myo*-inositol serves as a building block for glucuronic acid, which is formed via *myo*-inositol oxygenase (MIOX). This glucuronic acid then leads to the synthesis of UDP-glucuronic acid (UDP-GlcA) through the action of glucuronokinases (GLCAK) and UDP-sugar pyrophosphorylase (USP). UDP-GlcA is subsequently converted to various UDP-sugars by the action of enzymes such as UDP-D-apiose/UDP-D-xylose synthase (AXS), UDP-xylose synthase (UXS), UDP-D-xylose 4-epimerase (UXE), and UDP-D-glucuronate 4-epimerase (GAE). These UDP-sugars include UDP-arabinose, UDP-apiose, UDP-galacturonic acid, and UDP-xylose, all of which are important cell wall components and building blocks for pectin or hemicellulose (Figure 4). As depicted in Figures 2 and 4, sucrose, *myo*-inositol, and xylose were significantly higher in yellow genotypes compared to white genotypes. In addition, *MIPS*, *USP*, and *UXS* were also detected with a significantly higher expression in yellow compared to white genotypes (Figure 4; Table 5; Tables S5 and S6). Furthermore, *MIPS*, *UXE*, and *GAE* exhibited a significant negative correlation to starch in the yellow genotypes. In the white genotypes, *UXS* showed a negative correlation and *UXE* displayed a positive correlation with starch. Notably, only *AXS* showed a positive correlation with starch in the yellow genotypes in the pathways described above (Figure 4; Table 5; Tables S5 and S6). Collectively, yellow varieties seem to not significantly prefer the UGD pathway for glucuronic acid synthesis. However, the significantly higher abundance of *MIPS*, its negative correlation to starch, and the significantly higher abundance of *myo*-inositol, along with a higher expression of *USP* in yellow genotypes, support the hypothesis of a preferred UDP-D-glucuronic acid synthesis via the *myo*-inositol pathway. The observed negative correlation of *UXE* expression with starch, the negative correlation of *GAE* with starch, and the higher abundance of xylose in the yellow varieties studied here (Figures 2 and 4) further suggest that the re-direction of sucrose or G6P to the *myo*-inositol pathway in yellow-fleshed genotypes leads to an increased synthesis of pectin and hemicellulose building blocks.

Endres and Tenhaken (2009) reported that *A. thaliana miox1* and *miox2* knockout mutants show decreased incorporation of MIOX-derived sugars into cell wall polymers, while overexpression of *MIOX4* results in increased incorporation. Additionally, Oleszkiewicz et al. (2021) and Wang et al. (2021) hypothesized unknown signaling interactions between cell wall and carotenoid biosynthesis. Wang et al. (2021) silenced *psy1* and *psy2* in *Nicotiana benthamiana* and *Nicotiana tabacum* L. varieties and observed not only a massive decrease in carotenoid biosynthesis but also a negative effect on the expression of genes known to be involved in glucan, cellulose, pectin, and galacturonan biosynthesis. Oleszkiewicz et al. (2021) generated *psy2* mutants using CRISPR/Cas9 in carrot calli, and observed changes in the composition of arabinogalactan, pectin, and the extension in the cell walls of mutant plants.

Significant increase of pectin and hemicellulose building blocks in yellow-fleshed varieties underlines re-allocation of carbon toward cell wall biosynthesis

We asked the fundamental question if yellow cultivars allocate a greater proportion of their carbon to cell wall components in contrast to white varieties. To address this question, we measured cell wall components of the 20 most contrasting genotypes with respect to their root yellowness. Cellulose, the primary and most abundant component of plant cell walls, consists of D-Glucose units

© 2024 The Author(s).

1365313x, 2024, 4, Downloaded from https://onlinelibrary.wiley.com/doi/10.1111/tpj.16909 by Nigeria Hinari NPL, Wiley Online Library on [02/12/2024]. See the Terms and Conditions (https://onlinelibrary.wiley.com/terms-and-conditions) on Wiley Online Library for rules of use; OA articles are governed by the applicable Creative Commons License

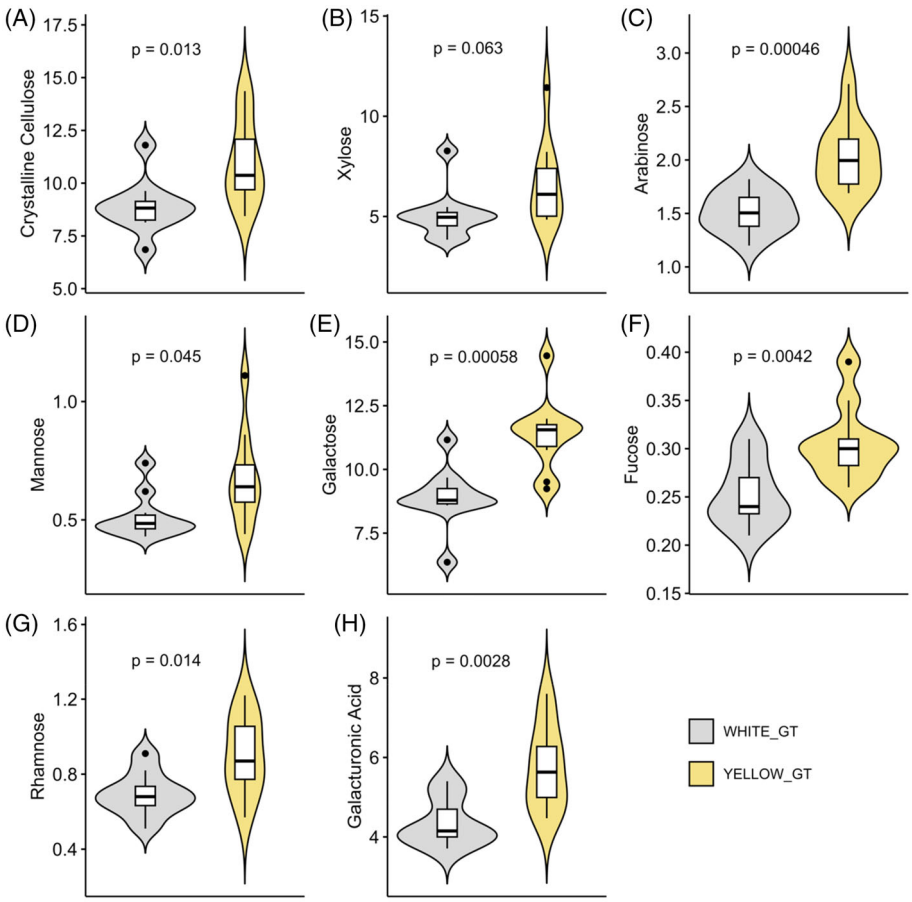

Figure 5. Measurement of cell wall components and comparison between the studied genotype groups.
Representation of cell wall component differences between white and yellow genotypes and corresponding significance. The 20 most contrasting genotypes (10 genotypes with highest and 10 with lowest carotenoid content) were used for cell wall measurement. *Y*-axis depicts the component amount in μg/mg dry weight. (A) Crystalline cellulose, (B) xylose, (C) arabinose, (D) mannose, (E) galactose, (F) fucose, (G) rhamnose, and (H) galacturonic acid.

linked by β(1,4)-glycosidic bonds, with crystalline cellulose structures containing up to 15 000 glucose units (Correa & Kruse, 2018; Polko & Kieber, 2019). Comparing the levels of crystalline cellulose in the analyzed genotypes, we observed a significant higher accumulation in yellow compared to white genotypes (Figure 5A). While cellulose is exclusively derived from glucose, matrix polysaccharides such as hemicelluloses and pectic polysaccharides are heteropolymers and often contain side chain substituents. The dominant hemicelluloses are largely composed of glucose, xylose, arabinose, mannose, galactose, and fucose (Pauly et al., 2013), while pectic polysaccharides contain galacturonic acid, rhamnose, and particularly, in tubers, galactose (Oxenbøll Sørensen et al., 2000). Comparing matrix polymer monosaccharides, we observed significantly higher abundance in yellow-fleshed cassava varieties for all but xylose ($P = 0.063$). We also observed significantly higher levels of pectic galacturonic acid and rhamnose (Figure 5B–H). During lignification, the cellulose/hemicellulose composite is penetrated by oxidative coupling of lignin monomers to form lignin to strengthen the cell wall (Barros et al., 2015). Lignin is a derivative of phenylpropanoids, which in turn derive from L-phenylalanine. Phenylalanine is cleaved from ammonia by phenylalanine ammonia lyase (PAL) to form cinnamic acid. This acid is converted by further enzymes to p-coumaryl coenzyme A, which is reduced to monolignol in the final step through cinnamyl alcohol dehydrogenase (CAD) (Wang et al., 2013). When the expression of the genes involved in lignin biosynthesis is examined, no difference in the expression of these genes between white and yellow genotypes was observed. Furthermore, there was no difference in phenylalanine levels between yellow and white genotypes detectable (Figure 3), which excludes the hypothesis of a significant increase in lignin levels in yellow genotypes.

© 2024 The Author(s).

1365313x, 2024, 4, Downloaded from https://onlinelibrary.wiley.com/doi/10.1111/tpj.16909 by Nigeria Hinari NPL, Wiley Online Library on [02/12/2024]. See the Terms and Conditions (https://onlinelibrary.wiley.com/terms-and-conditions) on Wiley Online Library for rules of use; OA articles are governed by the applicable Creative Commons License

Overall, these results support our hypothesis that yellow varieties have a recognizable tendency to divert a higher proportion of carbon resources for cell wall components at the expense of starch accumulation than their white counterparts. Given that we controlled for carotenoid levels as a confounding factor to isolate differences solely attributable to starch accumulation between the studied genotype groups, we hypothesize that the accumulation of wall components is a direct result of subcellular adjustments made for the accumulation of carotenoids, rather than an incidental pleiotropic consequence of metabolic pathways concurrently altered with carotenoid biosynthesis.

CONCLUSION

Photosynthates that have been transported to the sink organs of plants can be metabolized into various carbon compounds like starch, fatty acids, or cell wall components. The types and amounts of storage compounds differ significantly between plant species and genotypes and may heavily influence the value of the crop. Therefore, a key objective in many biotechnological approaches is to understand the mechanisms involved in carbon partitioning between metabolic pathways determining the final composition of the sink organ.

In this study, we investigated the differences in carbon partitioning between "white" and "yellow" cassava genotypes by analyzing a breeding panel containing 49 African cassava genotypes, with contrasting starch and carotenoid levels. With our experimental setup and analyses, we unified the three sources of data and were able to identify biochemical pathways that are linked to the crop's phenotype, metabolome, and transcriptome. In the genotypes under investigation, we examined a negative correlation between starch and carotenoid content, a metabolic separation between high-starch and high-carotenoid varieties, and a shift in gene expression from high-starch to high-carotenoid varieties. When taking the variety's carotenoid levels into account, we also observed a positive correlation of genes involved in starch biosynthesis and starch content in both, white and yellow genotypes. Only minor differences in expression of genes involved in *de novo* fatty acid biosynthesis between white and yellow genotypes and almost no correlation to starch of those genes was found. Importantly, we found a significantly higher abundance and negative correlation to starch of almost all genes and all metabolites associated with *myo*-inositol, raffinose, and the biosynthesis of building blocks for pectin and hemicellulose in yellow genotypes. Additionally, significantly higher levels of cell wall components were measured in the yellow-fleshed cassava genotypes. These results enhance our understanding of the factors influencing the trade-off among starch, carotenoids, and cell wall contents in cassava and will likely prove highly informative for future breeding strategies.

MATERIALS AND METHODS

Plant material, phenotyping, and harvest

The population used in this study is composed of 49 African cassava genotypes. The genotypes were planted as a preliminary yield trial in Ibadan (7°24′ N, 3°54′ E), Nigeria, from 2020 to 2021. Plots consisted of two rows with 10 plants per plot, in a randomized complete block design with two replications. Spacings between rows and plants were 1 and 0.8 m, respectively. Planting was performed from June to July 2020 and root harvesting was done at the same time the following year. Phenotyping was done for all 49 genotypes for traits related to biotic stress, storage root quality (e.g., dry matter, starch, and carotenoid content), and several other traits related to leaves, stems, and roots.

Sample preparation and RNA sequencing

For all 49 genotypes, storage root cross-sections of six replicates per plot were harvested and pooled for further processing. All root samples were packed in aluminum foil, transferred to liquid nitrogen, and stored at −80°C until further processing.

RNA was extracted from all 49 samples (first replication) using the Spectrum Plant Total RNA Kit. PolyA-selected library preparation and strand unspecific paired-end sequencing were provided as a custom service (Illumina NovaSeq 6000; Novogene, Cambridge, UK).

Metabolite measurements

The same material used for RNA extraction was used for metabolome analysis using gas chromatography–mass spectrometry (GC–MS) analysis and was processed as described in Rosado-Souza et al. (2019). Data were reported according to recently updated reporting standards for metabolomics (Alseekh et al., 2021; Table S2).

Cell wall component measurements

In order to test whether yellow cultivars allocate a different proportion of their carbon resources to cell wall components compared to white-fleshed varieties, we measured cell wall components for the 20 most contrasting carotenoid genotypes (10 genotypes showing the highest and 10 genotypes showing the lowest carotenoid content). Wall polysaccharide and de-starching were performed according to Oxenbøll Sørensen et al. (2000) in a scaled-down version. Milled and freeze-dried root material (150 mg) was re-suspended in 1.5 ml of ice-cold extraction buffer A [1% sodium deoxycholate (Sigma-Aldrich), 20 mM Hepes (Fisher Bioreagents) (pH 7.5), and 5 mM $Na_2S_2O_5$ (Fisher Chemical)]. After homogenization in a Retsch Mill MM400 (1 min 30 Hz), the suspension was centrifuged for 15 min at 4°C and 12 000 rpm (Eppendorf 5810 R). The supernatant was discarded, the pellet re-suspended in ice-cold extraction buffer B [0.5% sodium deoxycholate, 20 mM Hepes (pH 7.5), and 3 mM $Na_2S_2O_5$] and incubated for 30 min at 4°C shaking at 1000 rpm (Eppendorf Thermomix). The centrifugations and washes in buffer B were repeated three times with the final washing step overnight. The pellet was washed three times with 1 mL ice-cold Milli-Q water before resuspension in 1.5 mL PAW (phenol: acetic acid: water, 2:1:1 by volume) for 3 h at 22°C, with subsequent centrifugation for 20 min at 22°C and 12 000 rpm. After three washing steps with 1 ml Milli-Q water, the material was resuspended in 1.5 ml 25 mM NaOAc, pH 4.0, heated for 20 min at 80°C to gelatinize the starch, and cooled down on ice. The pH was adjusted to pH 5.0 by addition of 1 M

© 2024 The Author(s).

1365313x, 2024, 4, Downloaded from https://onlinelibrary.wiley.com/doi/10.1111/tpj.16909 by Nigeria Hinari NPL, Wiley Online Library on [02/12/2024]. See the Terms and Conditions (https://onlinelibrary.wiley.com/terms-and-conditions) on Wiley Online Library for rules of use; OA articles are governed by the applicable Creative Commons License

NaOH, and 40 μg α-amylase (*B. licheniformis*, Sigma-Aldrich), 0.4 U pullulanase (*B. licheniformis*, Megazyme), and 1 steel ball (Ø 5 mm) were added. The tubes were shaken horizontally at 225 rpm for 3 h at 37°C, followed by enzyme inactivation for 10 min at 80°C. The pellets were washed twice with water and the destarching step was repeated twice, followed by a final washing step with 1.5 ml acetone and drying at 40°C. The starch content in the residual material was quantified based on the Total Starch Kit protocol (K-TSTA, Megazyme) with modifications. The extracted and destarched material (1 mg) was treated with a thermostable α-amylase for 15 min at 100°C with inversion every 5 min and subsequent cooling on ice. Amyloglucosidase (50 μl) was added; the suspensions were mixed and incubated for 30 min at 50°C. The glucose content in the supernatant was quantified with the GOPOD method according to Kraemer et al. (2021). The monosaccharides of the matrix polysaccharides were hydrolyzed with 2 M TFA hydrolysis (Foster et al., 2010), followed by separation on a HPAEC System (Knauer Azura) according to (Wang et al., 2023). The crystalline cellulose content in the remaining TFA insoluble pellet was measured according to Foster et al. (2010). Measurements are reported in Table S7.

Data pre-processing

Since the linear relationship between the intensity of yellow color in cassava storage roots and the carotenoid content (Pearson's $r = 0.8$) is already well studied (Akinwale et al., 2010; Chávez et al., 2005; Iglesias et al., 1997; Sánchez et al., 2014), we used yellowness as a proxy for carotenoid content. To avoid subjectivity by measuring the yellowness visually, a chromameter was used to assess lightness (L^*), red and green (a^*, positive = red, negative = green), as well as yellow and blue (b^*, positive = yellow, negative = blue) color values using the Commission Internationale de l'Éclairage (CIELAB) method. Genotypes with a positive Chromameter $b^* \leq 25$ were identified as low-carotenoid content genotypes (referred to as white genotypes), whereas genotypes showing a $b^* > 25$ were classified as high-carotenoid content genotypes (referred to as yellow genotypes). In the whole manuscript, carotenoid content refers to the chromameter b^* values as a measure of carotenoid content. For starch content analyses, the percentage of starch per genotype analyzed with near-infrared (NIR) spectroscopy was used.

Bioinformatic analyses

Raw sequence reads were inspected using FastQC v.0.11.9 (Andrews, 2010) and MultiQC v.1.13 (Ewels et al., 2016). Using BBMap v.38.97 (Bushnell, 2014), the reads were filtered for N-reads, common contaminants, and known adaptor sequences, subsequently. Reads were additionally filtered based on read quality (≥30) and length (≥35). Quality reports for checking trimming success were generated using FastQC and MultiQC. Adapter- and quality-trimmed RNAseq reads were mapped to the *Manihot esculenta* v8.1 reference genome, using STAR (v.2.7.10a) (Dobin et al., 2013). *Manihot esculenta* v8.1 reference genome and corresponding annotations were downloaded from Phytozome (available under: https://phytozome-next.jgi.doe.gov/info/Mesculenta_v8_1) and served as reference genome during any analyses (Goodstein et al., 2012). Uniquely mapped transcriptomic reads were quantified at gene level using featureCounts v.2.0.3 (Liao et al., 2014).

For sequence analysis, a variant calling, including all genotypes, was performed using the BCFtools v.1.15.1 *caLL* function (Li, 2011). Subsequent filters were applied using VCFtools v.0.1.17 (Danecek et al., 2011). Filtering parameters were adjusted according to minimum quality (20), depth (≥60), minor allele frequency (0.05), maximum number of genotypes allowed with missing value for called position (10% percent), and biallelic single nucleotide polymorphisms (SNPs).

Differential expression analysis between white and yellow varieties was conducted using DESeq2 (Love et al., 2014) in R. DEGs were subsequently filtered for average gene-level quantified read depth of ≥10. Average read depth was calculated for white and yellow genotypes separately to avoid falsely excluding genes, which are solely expressed in either white or yellow genotypes. *P*-value adjustment was performed using the false discovery rate (FDR), accepting genes as significantly differentially expressed with a threshold of FDR ≤0.01.

Depth filtered (≥10), variance-stabilizing transformed high-quality reads were used to identify genes that are significantly correlated to starch, while controlling for carotenoid content as a confounding effect, in the white and the yellow genotypes separately by performing a partial correlation analysis using the ppcor package (Kim, 2015) in R. Partial correlation quantifies the degree of association between two variables (here, gene expression and starch content), while adjusting for potential confounding effects of a third variable (carotenoid content). In simpler terms, this can be understood as examining the relationship between gene expression and starch while holding carotenoid levels constant. Transcripts showing $P \leq 0.05$ and $r \geq |0.3|$ were considered to be significantly correlated. If transcriptional correlation to starch is mentioned in the manuscript, we are always referring to a correlation to starch including carotenoid content as a confounding variable. Subsequently, significantly correlated genes were used to perform a functional enrichment analysis using the one-sided Fisher's exact test provided in the clusterProfiler package (Yu et al., 2012) in R. Genes were functionally categorized using KEGG orthology (KO) terms. *Manihot esculenta* genes were described by their best *A. thaliana* hit based on BLASTP similarity. Pathway construction and identification of gene interactions were constructed through publications and publicly available literature and are listed in the corresponding sections.

For investigations including the metabolites, a *z*-score transformation of log values of the measured metabolites was performed and used for all subsequent analyses. Metabolites showing $P \leq 0.05$ and $r \geq |0.3|$ were accepted as being significantly correlated with starch.

All analyses outside of R were performed under Linux (Ubuntu v20.04.4). Analyses in R were performed under macOS (Catalina v10.15.7) and R version 4.1.0. For a detailed listing of all packages and corresponding versions used in R, see Data S1—R Session info. For visualization, if not otherwise specified, plots were generated using ggplot (Wickham, 2016) in R and finalized using Inkscape v1.0.2 (Inkscape, 2020).

AUTHOR CONTRIBUTIONS

WZ, US, and IYR designed the research. IYR and AMD designed and executed the field trials. AS processed the sample material. ARF and LRS conceived and performed the metabolic analyses. HEN and BP conceived and performed the sugar measurements. MP conceived and SR (HHU) performed the cell wall measurements. SG, DR, and SR (FAU) performed the analysis. WZ and US organized and supervised the work. SG wrote the manuscript with contributions of all authors. All authors have read and approved the submitted version of the manuscript.

© 2024 The Author(s).

1365313x, 2024, 4, Downloaded from https://onlinelibrary.wiley.com/doi/10.1111/tpj.16909 by Nigeria Hinari NPL, Wiley Online Library on [02/12/2024]. See the Terms and Conditions (https://onlinelibrary.wiley.com/terms-and-conditions) on Wiley Online Library for rules of use; OA articles are governed by the applicable Creative Commons License

ACKNOWLEDGMENTS

We thank Otilia Ciobotea and Michaela Reiser for their excellent technical assistance. US: received funding from the Bill and Melinda Gates Foundation through the grant INV-008053 (Cassava Source-Sink). MP: received funding from the Cluster of Excellence on Plant Sciences (CEPLAS) funded by the Deutsche Forschungsgemeinschaft (DFG, German Research Foundation) under Germany's Excellence Strategy—EXC 2048/1—Project ID: 390686111.

CONFLICT OF INTEREST

The authors have declared that no competing interest exists.

DATA AVAILABILITY STATEMENT

All used commands and scripts are available on GitHub (https://github.com/Division-of-Biochemistry-Publications/CASS). Raw sequencing reads have been deposited to NCBI's Sequence Read Archive (submission ID: SUB13965463) under BioProject ID PRJNA1039569, available at https://www.ncbi.nlm.nih.gov/sra/PRJNA1039569.

SUPPORTING INFORMATION

Additional Supporting Information may be found in the online version of this article.

Data S1. Supporting Information - Overview on Figures and Tables.

Figure S1. Chromosomal distribution of all detected significantly differential expressed genes between white and yellow genotypes across all 18 *Manihot esculenta* chromosomes.

Figure S2. Functional enrichment analysis for genes showing significant correlation with starch after correcting for carotenoid content as confounding effect.

Table S1. All measured metabolites and respective assignment as white or yellow variety.

Table S2. Metabolite reporting checklist.

Table S3. Genotype distribution for all genotypes for *PSY2* SNP position 31960252.

Table S4. List of all significant differentially expressed genes between white and yellow genotypes.

Table S5. Listing of all genes significantly correlated to starch (including carotenoid content as confounding effect) in one of the two genotype groups.

Table S6. Listing of all genes significantly differentially expressed between white and yellow genotypes, significantly correlated to starch in one of the genotype groups, or specifically mentioned in the main text of the manuscript.

Table S7. All measured cell wall monosaccharides and respective assignment as white or yellow variety.

REFERENCES

Adeniji, O.T., Odo, P.E. & Ibrahim, B. (2011) Genetic relationships and selection indices for cassava root yield in Adamawa state, Nigeria. *African Journal of Agricultural Research*, **6**(13), 2931–2934.

Akinwale, M.G., Aladesanwa, R.D., Akinyele, B.O., Dixon, A.G.O. & Odiyi, A.C. (2010) Inheritance of ß-carotene in cassava (*Manihot esculenta* crantza). *International Journal of Genetics and Molecular Biology*, **2**, 198–201.

Alseekh, S., Aharoni, A., Brotman, Y., Contrepois, K., D'Auria, J., Ewald, J. *et al.* (2021) Mass spectrometry-based metabolomics: a guide for annotation, quantification and best reporting practices. *Nature Methods*, **18**(7), 747–756.

Andrews, S.R. (2010) *FastQC*. Available at: http://www.bioinformatics.babraham.ac.uk/projects/fastqc/

Awotide, B., Abdoulaye, T., Alene, A. & Manyong, V.M. (2014) Assessing the extent and determinants of adoption of improved cassava varieties in south-western Nigeria. *Journal of Development and Agricultural Economics*, **6**(9), 376–385.

Barros, J., Serk, H., Granlund, I. & Pesquet, E. (2015) The cell biology of lignification in higher plants. *Annals of Botany*, **115**(7), 1053–1074.

Beyene, G., Solomon, F.R., Chauhan, R.D., Gaitán-Solis, E., Narayanan, N., Gehan, J. *et al.* (2018) Provitamin A biofortification of cassava enhances shelf life but reduces dry matter content of storage roots due to altered carbon partitioning into starch. *Plant Biotechnology Journal*, **16**(6), 1186–1200.

Bushnell, B. (2014) *BBMap short read aligner, and other bioinformatic tools*. Available at: https://sourceforge.net/projects/bbmap/

Cai, J., Xue, J., Zhu, W., Luo, X., Lu, X., Xue, M. *et al.* (2023) Integrated metabolomic and transcriptomic analyses reveals sugar transport and starch accumulation in two specific germplasms of *Manihot esculenta* Crantz. *International Journal of Molecular Sciences*, **24**(8), 7236.

Carvalho, L.J., Filho, J.F., Anderson, J.V., Figueiredo, P.W. & Chen, S. (2018) Storage Root of Cassava: Morphological Types, Anatomy, Formation, Growth, Development and Harvest Time. In: Waisundara, V. (Ed.) *Cassava*. Intertech Open.

Chavez, A.L., Bedoya, J.M., Sánchez, T., Iglesias, C., Ceballos, H. & Roca, W. (2000) Iron, carotene, and ascorbic acid in cassava roots and leaves. *Food and Nutrition Bulletin*, **21**(4), 410–413.

Chávez, A.L., Sánchez, T., Jaramillo, G., Bedoya, J.M., Echeverry, J., Bolaños, E.A. *et al.* (2005) Variation of quality traits in cassava roots evaluated in landraces and improved clones. *Euphytica*, **143**(1–2), 125–133.

Correa, C.R. & Kruse, A. (2018) Supercritical water gasification of biomass for hydrogen production–review. *The Journal of Supercritical Fluids*, **133**, 573–590.

Danecek, P., Auton, A., Abecasis, G., Albers, C.A., Banks, E., DePristo, M.A. *et al.* (2011) The variant call format and VCFtools. *Bioinformatics*, **27**(15), 2156–2158.

Dobin, A., Davis, C.A., Schlesinger, F., Drenkow, J., Zaleski, C., Jha, S. *et al.* (2013) STAR: Ultrafast universal RNA-seq aligner. *Bioinformatics*, **29**(1), 15–21.

Elango, D., Rajendran, K., Van der Laan, L., Sebastiar, S., Raigne, J., Thaiparambil, N.A. *et al.* (2022) Raffinose family oligosaccharides: friend or foe for human and plant health? *Frontiers in Plant Science*, **13**, 829118.

Endres, S. & Tenhaken, R. (2009) Myoinositol oxygenase controls the level of Myoinositol in Arabidopsis, but does not increase ascorbic acid. *Plant Physiology*, **149**(2), 1042–1049.

Esuma, W., Herselman, L., Labuschagne, M.T., Ramu, P., Lu, F., Baguma, Y. *et al.* (2016) Genome-wide association mapping of provitamin A carotenoid content in cassava. *Euphytica*, **212**(1), 97–110.

Ewels, P., Magnusson, M., Lundin, S. & Käller, M. (2016) MultiQC: summarize analysis results for multiple tools and samples in a single report. *Bioinformatics*, **32**(19), 3047–3048.

FAO. (2023) *Crops and livestock products*. Available at: https://www.fao.org/faostat/en/#data/QCL

Figueroa, C.M., Asencion Diez, M.D., Ballicora, M.A. & Iglesias, A.A. (2022) Structure, function, and evolution of plant ADP-glucose pyrophosphorylase. *Plant Molecular Biology*, **108**(4–5), 307–323.

Foster, C.E., Martin, T.M. & Pauly, M. (2010) Comprehensive compositional analysis of plant cell walls (lignocellulosic biomass) part II: carbohydrates. *Journal of Visualized Experiments*, **37**, e1837.

Fraser, P.D., Enfissi, E.M.A., Halket, J.M., Truesdale, M.R., Yu, D., Gerrish, C. *et al.* (2007) Manipulation of phytoene levels in tomato fruit: Effects on isoprenoids, plastids, and intermediary metabolism. *The Plant Cell*, **19**(10), 3194–3211. Available from: https://doi.org/10.1105/tpc.106.049817

Goodstein, D.M., Shu, S., Howson, R., Neupane, R., Hayes, R.D., Fazo, J. *et al.* (2012) Phytozome: a comparative platform for green plant genomics. *Nucleic Acids Research*, **40**(D1), D1178–D1186.

Guschina, I.A. & Harwood, J.L. (2007) Complex lipid biosynthesis and its manipulation in plants. In: Ranalli, P. (Ed.) *Improvement of Crop Plants for Industrial End Uses*. Dordrecht, Netherlands: Springer, pp. 253–279.

© 2024 The Author(s).

1365313x, 2024, 4, Downloaded from https://onlinelibrary.wiley.com/doi/10.1111/tpj.16909 by Nigeria Hinari NPL, Wiley Online Library on [02/12/2024]. See the Terms and Conditions (https://onlinelibrary.wiley.com/terms-and-conditions) on Wiley Online Library for rules of use; OA articles are governed by the applicable Creative Commons License

Harwood, J.L. (1996) Recent advances in the biosynthesis of plant fatty acids. *Biochimica et Biophysica Acta (BBA)—Lipids and Lipid Metabolism*, **1301**(1–2), 7–56.

Hefferon, K. (2015) Nutritionally enhanced food crops; Progress and perspectives. *International Journal of Molecular Sciences*, **16**(2), 3895–3914.

Iglesias, C., **Mayer, J.**, **Chavez, L.** & **Calle, F.** (1997) Genetic potential and stability of carotene content in cassava roots. *Euphytica*, **94**(3), 367–373.

Inkscape. (2020) *Inkscape*. Available at: https://inkscape.org/release/inkscape-1.2.2/

Jonik, C., **Sonnewald, U.**, **Hajirezaei, M.R.**, **Flügge, U.I.** & **Ludewig, F.** (2012) Simultaneous boosting of source and sink capacities doubles tuber starch yield of potato plants. *Plant Biotechnology Journal*, **10**(9), 1088–1098.

Kanwal, F., **Ren, D.**, **Kanwal, W.**, **Ding, M.**, **Su, J.** & **Shang, X.** (2023) The potential role of nondigestible Raffinose family oligosaccharides as prebiotics. *Glycobiology*, **33**(4), 274–288.

Ke, J., **Behal, R.H.**, **Back, S.L.**, **Nikolau, B.J.**, **Wurtele, E.S.** & **Oliver, D.J.** (2000) The role of pyruvate dehydrogenase and acetyl-coenzyme A Synthetase in fatty acid synthesis in developing Arabidopsis seeds. *Plant Physiology*, **123**(2), 497–508.

Keller, I., **Müdsam, C.**, **Rodrigues, C.M.**, **Kischka, D.**, **Zierer, W.**, **Sonnewald, U.** ***et al.*** (2021) Cold-triggered induction of ROS- and Raffinose metabolism in freezing-sensitive taproot tissue of sugar beet. *Frontiers in Plant Science*, **12**, 715767.

Kim, S. (2015) Ppcor: An R package for a fast calculation to semi-partial correlation coefficients. *Communications for Statistical Applications and Methods*, **22**(6), 665–674.

Klaus, D., **Ohlrogge, J.B.**, **Neuhaus, H.E.** & **Dörmann, P.** (2004) Increased fatty acid production in potato by engineering of acetyl-CoA carboxylase. *Planta*, **219**(3), 389–396.

Klotke, J., **Kopka, J.**, **Gatzke, N.** & **Heyer, A.G.** (2004) Impact of soluble sugar concentrations on the acquisition of freezing tolerance in accessions of *Arabidopsis thaliana* with contrasting cold adaptation - evidence for a role of raffinose in cold acclimation: cold acclimation of Arabidopsis accessions. *Plant, Cell & Environment*, **27**(11), 1395–1404.

Kraemer, F.J., **Lunde, C.**, **Koch, M.**, **Kuhn, B.M.**, **Ruehl, C.**, **Brown, P.J.** ***et al.*** (2021) A mixed-linkage (1, 3; 1, 4)-β-D-glucan specific hydrolase mediates dark-triggered degradation of this plant cell wall polysaccharide. *Plant Physiology*, **185**(4), 1559–1573.

Lamm, C.E., **Rabbi, I.Y.**, **Medeiros, D.B.**, **Rosado-Souza, L.**, **Pommerrenig, B.**, **Dahmani, I.** ***et al.*** (2023) Efficient sugar utilization and transition from oxidative to substrate-level phosphorylation in high starch storage roots of African cassava genotypes. *The Plant Journal*, **tpj.16357**, 38–57.

Li, H. (2011) A statistical framework for SNP calling, mutation discovery, association mapping and population genetical parameter estimation from sequencing data. *Bioinformatics*, **27**(21), 2987–2993.

Liao, Y., **Smyth, G.K.** & **Shi, W.** (2014) featureCounts: An efficient general purpose program for assigning sequence reads to genomic features. *Bioinformatics*, **30**(7), 923–930.

Loewus, F.A. & **Loewus, M.W.** (1983) Myo-inositol: its biosynthesis and metabolism. *Annual Review of Plant Physiology*, **34**(1), 137–161.

Loewus, F.A. & **Murthy, P.P.N.** (2000) Myo-inositol metabolism in plants. *Plant Science*, **150**(1), 1–19.

Love, M.I., **Huber, W.** & **Anders, S.** (2014) Moderated estimation of fold change and dispersion for RNA-seq data with DESeq2. *Genome Biology*, **15**(12), 550.

Luo, X., **An, F.**, **Xue, J.**, **Zhu, W.**, **Wei, Z.**, **Ou, W.** ***et al.*** (2023) Integrative analysis of metabolome and transcriptome reveals the mechanism of color formation in cassava (*Manihot esculenta* Crantz) leaves. *Frontiers in Plant Science*, **14**, 1181257.

Mehdi, R., **Lamm, C.E.**, **Bodampalli Anjanappa, R.**, **Müdsam, C.**, **Saeed, M.**, **Klima, J.** ***et al.*** (2019) Symplasmic phloem unloading and radial post-phloem transport via vascular rays in tuberous roots of *Manihot esculenta*. *Journal of Experimental Botany*, **70**(20), 5559–5573.

Morsy, M.R., **Jouve, L.**, **Hausman, J.-F.**, **Hoffmann, L.** & **Stewart, J.M.D.** (2007) Alteration of oxidative and carbohydrate metabolism under abiotic stress in two rice (*Oryza sativa* L.) genotypes contrasting in chilling tolerance. *Journal of Plant Physiology*, **164**(2), 157–167.

Munyikwa, T.R.I., **Langeveld, S.**, **Salehuzzaman, S.N.I.M.**, **Jacobsen, E.** & **Visser, R.G.F.** (1997) Cassava starch biosynthesis: new avenues for modifying starch quantity and quality. *Euphytica*, **96**(1), 65–75.

Nassar, N. & **Ortiz, R.** (2010) Breeding cassava to feed the poor. *Scientific American*, **302**(5), 78–84.

Njoku, D.N., **Gracen, V.E.**, **Offei, S.K.**, **Asante, I.K.**, **Egesi, C.N.**, **Kulakow, P.** ***et al.*** (2015) Parent-offspring regression analysis for total carotenoids and some agronomic traits in cassava. *Euphytica*, **206**(3), 657–666.

Ntawuruhunga, P. & **Dixon, A.G.** (2010) Quantitative variation and interrelationship between factors influencing cassava yield. *Journal of Applied Biosciences*, **26**(4), 1594–1602.

Ogbonna, A.C., **Ramu, P.**, **Esuma, W.**, **Nandudu, L.**, **Morales, N.**, **Powell, A.** ***et al.*** (2021) A population based expression atlas provides insights into disease resistance and other physiological traits in cassava (*Manihot esculenta* Crantz). *Scientific Reports*, **11**(1), 23520.

Olayide, P., **Alexandersson, E.**, **Tzfadia, O.**, **Lenman, M.**, **Gisel, A.** & **Stavolone, L.** (2023) Transcriptome and metabolome profiling identify factors potentially involved in pro-vitamin A accumulation in cassava landraces. *Plant Physiology and Biochemistry*, **199**, 107713.

Oleszkiewicz, T., **Klimek-Chodacka, M.**, **Kruczek, M.**, **Godel-Jędrychowska, K.**, **Sala, K.**, **Milewska-Hendel, A.** ***et al.*** (2021) Inhibition of carotenoid biosynthesis by CRISPR/Cas9 triggers Cell Wall Remodelling in carrot. *International Journal of Molecular Sciences*, **22**(12), 6516.

Oxenbøll Sørensen, S., **Pauly, M.**, **Bush, M.**, **Skjøt, M.**, **McCann, M.C.**, **Borkhardt, B.** ***et al.*** (2000) Pectin engineering: modification of potato pectin by in vivo expression of an endo-1, 4-β-D-galactanase. *Proceedings of the National Academy of Sciences of the United States of America*, **97**(13), 7639–7644.

Pauly, M., **Gille, S.**, **Liu, L.**, **Mansoori, N.**, **de Souza, A.**, **Schultink, A.** ***et al.*** (2013) Hemicellulose biosynthesis. *Planta*, **238**, 627–642.

Polko, J.K. & **Kieber, J.J.** (2019) The regulation of cellulose biosynthesis in plants. *The Plant Cell*, **31**(2), 282–296.

Rabbi, I.Y., **Kayondo, S.I.**, **Bauchet, G.**, **Yusuf, M.**, **Aghogho, C.I.**, **Ogunpaimo, K.** ***et al.*** (2022) Genome-wide association analysis reveals new insights into the genetic architecture of defensive, agro-morphological and quality-related traits in cassava. *Plant Molecular Biology*, **109**(3), 195–213.

Rabbi, I.Y., **Udoh, L.I.**, **Wolfe, M.**, **Parkes, E.Y.**, **Gedil, M.A.**, **Dixon, A.** ***et al.*** (2017) Genome-wide association mapping of correlated traits in cassava: dry matter and Total carotenoid content. *The Plant Genome*, **10**(3).

Rawsthorne, S. (2002) Carbon flux and fatty acid synthesis in plants. *Progress in Lipid Research*, **41**(2), 182–196.

Rodríguez-Villalón, A., **Gas, E.** & **Rodríguez-Concepción, M.** (2009) Phytoene synthase activity controls the biosynthesis of carotenoids and the supply of their metabolic precursors in dark-grown Arabidopsis seedlings. *The Plant Journal*, **60**(3), 424–435.

Rosado-Souza, L., **David, L.C.**, **Drapal, M.**, **Fraser, P.D.**, **Hofmann, J.**, **Klemens, P.A.W.** ***et al.*** (2019) Cassava metabolomics and starch quality. *Current Protocols in Plant Biology*, **4**(4).

Rüscher, D., **Vasina, V.V.**, **Knoblauch, J.**, **Bellin, L.**, **Pommerrenig, B.**, **Alseekh, S.** ***et al.*** (2024) Symplasmic phloem loading and subcellular transport in storage roots are key factors for carbon allocation in cassava. *Plant Physiology*, kiae298. Online ahead of print. Available from: https://doi.org/10.1093/plphys/kiae298

Sánchez, T., **Ceballos, H.**, **Dufour, D.**, **Ortiz, D.**, **Morante, N.**, **Calle, F.** ***et al.*** (2014) Prediction of carotenoids, cyanide and dry matter contents in fresh cassava root using NIRS and hunter color techniques. *Food Chemistry*, **151**, 444–451.

Sanyal, R., **Kumar, S.**, **Pattanayak, A.**, **Kar, A.** & **Bishi, S.K.** (2023) Optimizing raffinose family oligosaccharides content in plants: A tightrope walk. *Frontiers in Plant Science*, **14**, 1134754.

Talsma, E.F., **Borgonjen-van Den Berg, K.J.**, **Melse-Boonstra, A.**, **Mayer, E.V.**, **Verhoef, H.**, **Demir, A.Y.** ***et al.*** (2018) The potential contribution of yellow cassava to dietary nutrient adequacy of primary-school children in eastern Kenya; the use of linear programming. *Public Health Nutrition*, **21**(2), 365–376.

Wang, S., **Robertz, S.**, **Seven, M.**, **Kraemer, F.**, **Kuhn, B.M.**, **Liu, L.** ***et al.*** (2023) A large-scale forward genetic screen for maize mutants with altered lignocellulosic properties. *Frontiers in Plant Science*, **14**, 1099009.

Wang, Y., **Chantreau, M.**, **Sibout, R.** & **Hawkins, S.** (2013) Plant cell wall lignification and monolignol metabolism. *Frontiers in Plant Science*, **4**, 51659.

Wang, Z., **Zhang, L.**, **Dong, C.**, **Guo, J.**, **Jin, L.**, **Wei, P.** ***et al.*** (2021) Characterization and functional analysis of phytoene synthase gene family in tobacco. *BMC Plant Biology*, **21**(1), 32.

© 2024 The Author(s).

1365313x, 2024, 4, Downloaded from https://onlinelibrary.wiley.com/doi/10.1111/tpj.16909 by Nigeria Hinari NPL, Wiley Online Library on [02/12/2024]. See the Terms and Conditions (https://onlinelibrary.wiley.com/terms-and-conditions) on Wiley Online Library for rules of use; OA articles are governed by the applicable Creative Commons License

Welsch, R., **Arango, J.**, **Bär, C.**, **Salazar, B.**, **Al-Babili, S.**, **Beltrán, J.** ***et al.*** (2010) Provitamin A accumulation in cassava (*Manihot esculenta*) roots driven by a single nucleotide polymorphism in a phytoene synthase gene. *The Plant Cell*, **22**(10), 3348–3356.

Wickham, H. (2016) *ggplot2: Elegant Graphics for Data Analysis*, 2nd edition. Cham, Switzerland: Springer.

Wilson, M.C., **Mutka, A.M.**, **Hummel, A.W.**, **Berry, J.**, **Chauhan, R.D.**, **Vijayaraghavan, A.** ***et al.*** (2017) Gene expression atlas for the food security crop cassava. *New Phytologist*, **213**(4), 1632–1641.

Wright, L.P., **Rohwer, J.M.**, **Ghirardo, A.**, **Hammerbacher, A.**, **Ortiz-Alcaide, M.**, **Raguschke, B.** ***et al.*** (2014) Deoxyxylulose 5-phosphate synthase controls flux through the methylerythritol 4-phosphate pathway in Arabidopsis. *Plant Physiology*, **165**(4), 1488–1504.

Xiao, L., **Cao, S.**, **Shang, X.**, **Xie, X.**, **Zeng, W.**, **Lu, L.** ***et al.*** (2021) Metabolomic and transcriptomic profiling reveals distinct nutritional properties of cassavas with different flesh colors. *Food Chemistry: Molecular Sciences*, **2**, 100016.

Yan, S., **Liu, Q.**, **Li, W.**, **Yan, J.** & **Fernie, A.R.** (2022) Raffinose family oligosaccharides: crucial regulators of plant development and stress responses. *Critical Reviews in Plant Sciences*, **16**(5), 284–287.

Yu, G., **Wang, L.-G.**, **Han, Y.** & **He, Q.-Y.** (2012) clusterProfiler: An R package for comparing biological themes among gene clusters. *OMICS: A Journal of Integrative Biology*, **16**(5), 284–287.

Zeeman, S.C., **Kossmann, J.** & **Smith, A.M.** (2010) Starch: its metabolism, evolution, and biotechnological modification in plants. *Annual Review of Plant Biology*, **61**(1), 209–234.

Zhang, L., **Häusler, R.E.**, **Greiten, C.**, **Hajirezaei, M.R.**, **Haferkamp, I.**, **Neuhaus, H.E.** ***et al.*** (2008) Overriding the co-limiting import of carbon and energy into tuber amyloplasts increases the starch content and yield of transgenic potato plants. *Plant Biotechnology Journal*, **6**(5), 453–464.

© 2024 The Author(s).

1365313x, 2024, 4, Downloaded from https://onlinelibrary.wiley.com/doi/10.1111/tpj.16909 by Nigeria Hinari NPL, Wiley Online Library on [02/12/2024]. See the Terms and Conditions (https://onlinelibrary.wiley.com/terms-and-conditions) on Wiley Online Library for rules of use; OA articles are governed by the applicable Creative Commons License